Distinct Surface Morphologies of Electropolymerized Polymethylsiloxane Network Polypyrrole and Comonomer Films

Prasad Taranekar, Xiaowu Fan, and Rigoberto Advincula*,†

Department of Chemistry, University of Alabama at Birmingham, Birmingham, Alabama 35294, and Department of Chemistry, University of Houston, Houston, Texas 77204

Received January 9, 2002. In Final Form: July 26, 2002

The electropolymerization of polysiloxane-functionalized pyrrole or poly(methyl-(undec-pyrrole-1-yl-decyl)-siloxane), to form conjugated network polymer films, is described. The "precursor polypyrrole" was electropolymerized using dynamic cyclic voltammetry (CV) on a flat conducting substrate electrode, resulting in cross-linked polypyrrole films. Unique "nanoscale" morphologies were formed because of phase-segregation of polysiloxane domains and cross-linked polypyrrole, depending on the thickness and electrochemical conditions. By electropolymerizing the precursor polymer in-situ with pyrrole comonomers, the morphology changes with composition ratio. The film properties were investigated by cyclic voltammetry (CV), FT-IR, UV−vis, atomic force microscopy (AFM), surface plasmon spectroscopy (SPS), and X-ray photoelectron spectroscopy (XPS). The precursor method extends the possibility of tailoring film properties of polypyrrole and other conjugated polymers. Interesting insights on the electrochemical properties of cross-linked electrodeposited conjugated polymer films are discussed.

Introduction

Polypyrroles (PPy's) have attracted much attention as electrically conducting polymers because of their high conductivity and stability.[1] Many investigations have been performed to study their preparation,[2] characterization,[3] and applications as electrical and electro-optical materials.[4] A characteristic feature for thin film electrochromic display applications is their intrinsic switching time, that is, between insulating and conducting states under electrochemical conditions.[5] Since conductivity depends on electrolyte anion doping, which in turn is potential dependent,[6] the electrode potential becomes important. PPy thin films can be switched reversibly between conducting and insulating states as a function of potential, making them good candidates for electronic switching devices.[7] The application of PPy films to thin organic electroluminescent display devices has also been reported.[4d] While there is a large interest in thin film applications of PPy, very few studies have been performed relating these properties with morphology as ultrathin films.[8] Several groups have used self-assembled monolayers (SAMs) to modify electrodes and the electropolymerization process, resulting in different film morphologies.[9] The Knoll group and our group have focused on in-situ opto-electrochemical investigations of conducting polymer ultrathin films in relation to their morphological properties using surface plasmon spectroscopy (SPS).[10] We have found that morphology is important not only in the electrochemical process but also for their optical properties.

Recently, we have reported a novel method of depositing high optical quality ultrathin films of conjugated polymers on flat electrode substrates such as indium tin oxide (ITO)[11] and Au.[11,12,16] Using a "precursor polymer" route, conju-

† University of Houston.

(1) (a) Diaz, A. F.; Kanazawa, K. K.; Gardini, G. P. *J. Chem. Soc., Chem. Commun.* **1979**, 635. (b) Skotheim, T. A., Ed. *Handbook of conducting polymers*; Marcel Dekker: New York, 1986; Vol. 1, p 82. (c) Asavapiriyanont, S.; Chandler, G. K.; Gunawardena, G. A.; Pletcher, D. *J. Electroanal. Chem.* **1984**, *177*, 245. (d) Heinze, J. *Synth. Met.* **1991**, *41*, 2805.

(2) Asavapiriyanont, S.; Chandler, G. K.; Gunawardena, G. A.; Pletcher, D. *J. Electroanal. Chem.* **1984**, *177*, 229.

(3) (a) Earlandson, R.; Inganas, O.; Lunstrom, I.; Salaneck, W. R. *Synth. Met.* **1985**, *10*, 303. (b) De Paoli, M. A.; Peres, P. C. D.; Panero, S.; Scrosati, B. *Electrochim. Acta* **1992**, *37*, 1773.

(4) (a) Keda, O.; Okabayashi, K.; Tamura, H. *Chem Lett.* **1983**, 1821. (b) Lyons, M. E. G.; Breen, W.; Cassidy, J. *J. Chem. Soc., Faraday Trans.* **1991**, *87*, 115. (c) Lee, J. Y.; Ong, L. H.; Chuahi, G. K. *J. Appl. Electrochem.* **1992**, *221*, 738. (d) Park, J.; Lee, J.-H.: Lee, J.-Y.; Kho, S.; Kim, T.-W. *Thin Solid Films* **2000**, *363*, 259.

(5) Abranates, L. M.; Mesquita, J. C. *J. Electroanal. Chem.* **1991**, *307*, 275.

(6) (a) Feldberg, S. W. *J. Am. Chem. Soc.* **1984**, *106*, 4671. (b) Ko, J. M.; Rhee, H. W.; Park, S. M.; Kim, C. Y. *J. Electrochem. Soc.* **1990**, *137*, 905.

(7) (a) Riley, P. J.; Wallace, G. G. *J. Intell. Mater. Syst. Struct.* **1991**, *2*, 228. (b) Pyo, M.; Reynolds, J.; Warren, L.; Marcy, H. *Synth. Met.* **1994**, *68*, 71. (c) Schottland, P.; Zong, K.; Gaupp, C.; Thompson, B.; Thomas, C.; Giurgiu, I.; Hickman, R.; Abboud, K.; Reynolds, J. *Macromolecules* **2000**, *33*, 7051.

(8) Smela, E.; Gadegaard, N. *J. Phys. Chem. B* **2001**, *105*, 9395.

(9) (a) Simon, R. A.; Ricco, A. J.; Wrighton, M. S. *J. Am. Chem. Soc.* **1982**, *104*, 2031. (b) Kowalik, J.; Tolbert, L.; Ding, Y.; Bottomley, L.; Vogt, K.; Kohl, P. *Synth. Met.* **1993**, *55*, 1171. (c) Rubinstein, I.; Rishpon, J.; Sabatini, E.; Redondo, A.; Gottesfeld, S. *J. Am. Chem. Soc.* **1987**, *112*, 6135. (d) Willicut, R. J.; McCarley, R. L. *Langmuir* **1995**, *11*, 296. Willicut, R. J.; McCarley, R. L. *J. Am. Chem. Soc.* **1994**, *116*, 10823. (e) Sayre, C. N.; Collard, D. M. *Langmuir* **199**5, *11*, 302. (f) Sayre, C.; Collard D. *Langmuir* **1997**, *13*, 714. (g) Li, D.; Ding, W.; Wang, X.; Lu, L.; Yang, X. *Appl. Surf. Sci.* **2001**, *183*, 259.

(10) (a) Baba, A.; Advincula, R.; Knoll, W. *Polym. Mater. Sci. Eng. Prepr.* **2001**, *84*, 674. (b) Baba, A.; Advincula, R.; Knoll, W. *J. Phys. Chem. B* **2002**, *106*, 1581. (c) Xia, C.; Advincula, R. C.; Baba, A.; Knoll, W. *Langmuir* **2002**, *18*, 3555. (d) Baba, A.; Advincula, R.; Knoll, W. *Langmuir* **2002**, *18*, 4648−4652.

(11) (a) Xia, C.; Advincula, R.; Inaoka, S. *Polym. Prepr.* **2000**, *41*, 846. (b) Xia, C.; Advincula, R.; Inaoka, S. *Polym. Prepr.* **2000**, *41*, 859. (c) Inaoka, S.; Roitman, D.; Advincula, R. *Polym. Prepr.* **2000**, *41*, 808. (d) Advincula, R.; Xia, C.; Inaoka, S.; Roitman, D. Chapter review to *Thin Films*. In *Ultrathin Films of Conjugated Polymers on Conducting Surfaces*; Soriaga, M., Ed.; in press. (e) Inaoka, S.; Roitman, R.; Advincula, R. In *Forefront of Lithographic Materials Research*; Ito, H., Khojasteh, M., Li, W., Eds.; 2001; pp 239−245.

(12) (a) Onishi, K.; Advincula, R. *Polym. Mater. Sci. Eng. Prepr.* **2002**, *86*, 259. (b) Onishi, K.; Karim, S. A.; Nakai, T.; Masuda, T.; Advincula, R. *Polym. Prepr.* (*Am. Chem. Soc., Div. Polym. Chem.*) **2002**, *43*, 171.

(13) Clarson, S.; Fitzgerald, J.; Smith, S.; Owen, M. *Silicones and Silicone modified materials*; American Chemical Society: Washington, DC, 2000 (distributed by Oxford University Press).

10.1021/la025517y CCC: $22.00
Published on Web 08/30/2002

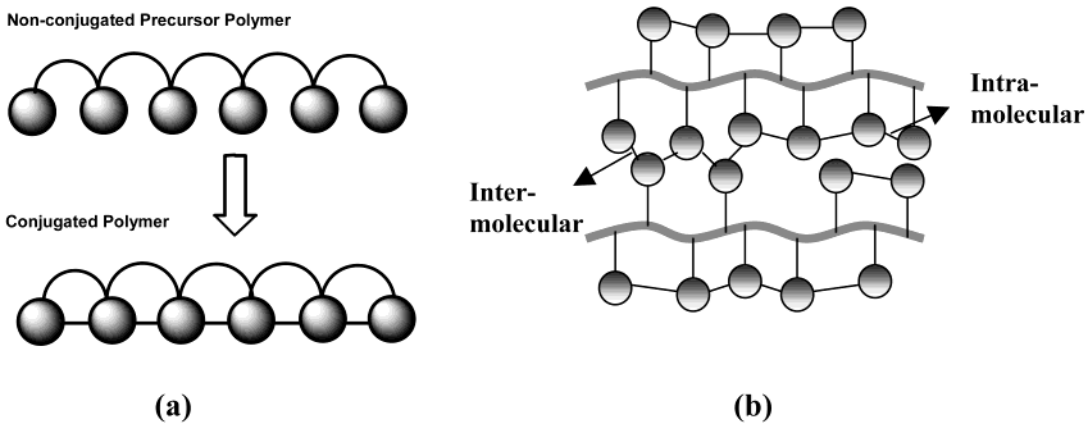

Figure 1. Precursor polymer concept for the synthesis of conjugated polymer networks: synthesis and cross-linking reactions.

gated network films were deposited and patterned by electrochemical methods for polymer light emitting diode (PLED) devices.[11e] In this approach, a polymer precursor is first synthesized and by design contains pendant electroactive monomer units (Figure 1a). Electropolymerization or chemical oxidation results in a network conjugated polymer having both inter- and intramolecular cross-linking possibilities (Figure 1b). The films are characterized by high optical quality (transparency), uniform coverage, good adhesion, smoothness in morphology, and control of dopant ion permeability.[11,12,16a] By controlling the amount of conjugated species and doping, it should be possible to control electrical conductivity.[12] The process is interesting for depositing *insoluble* conjugated polymer network ultrathin films for practical electro-optical applications. A number of combinations are possible with the precursor polymer backbone (nonconjugated and conjugated) and "electroactive monomer" side group. It is also possible to *copolymerize* the precursor polymer in-situ with small molecule electroactive comonomers, for example thiophene, pyrrole, aniline, and so forth.

In this study, we investigated the use of poly(methylhydrosiloxane) (PMHS) as a polymer backbone for polypyrrole network formation. These polymeric organic siloxanes or silicones consist of alternating silicon−oxygen (Si−O) units, making them flexible and hydrophobic polymers.[13] Properties include low surface tension, water repellence, high dielectric constant, gas permeability, thermal stability, inertness, and low glass transition temperatures, T_g.[13] Cross-linking of these polymers lead to gel- and rubber-like bulk solids. The PMHS polymer was grafted with electroactive pyrrole pendant groups through a hydrosilation reaction, forming poly(methyl-(undec-pyrrole-1-yl-decyl)-siloxane).[16] Electropolymerization was utilized to cross-link and deposit a conjugated network polypyrrole film to an electrode surface such as ITO or Au. Unique morphologies for a polypyrrole film were observed depending on thickness, composition ratio, substrate, and electrochemical conditions. Interesting insights were obtained on the electrochemical properties of cross-linked electrodeposited polymer films. This paper describes the synthesis, film preparation, electrochemical studies, comonomer composition ratio studies, and surface characterization of these unique films.

(14) Knoll, W. *Annu. Rev. Phys. Chem.* **1998**, *49*, 569.
(15) Bartlet, P. N.; Chung, Y. L.; Moore, P. *Electrochim. Acta* **1990**, *35*, 1051.
(16) (a) Xia, C.; Fan, X.; Park, M.; Advincula, R. *Langmuir* **2001**, *17*, 7893. (b) Gunaydin, O.; Toppare, L.; Yagci, Y.; Harabagiu, V.; Pintela, M.; Simionescu, B. *Polym. Bull.* **2002**, *47*, 501.

Experimental Section

Instrumentation. NMR spectra were recorded on a Bruker ARX 300 spectrometer with chloroform-*d* as solvent and tetramethylsilane (TMS) as internal standard. UV−vis spectra were recorded on a Hewlett-Packard 8453 spectrometer; cyclic voltammetry (CV) was performed on an Amel 2049 potentiostat and power lab/4SP system with a three-electrode cell. Size exclusion chromatography (SEC) experiments were done using a Waters 410 with a differential refractrometer and polystyrene calibration standards. Atomic force microscopy (AFM) imaging was done in air using a PicoScan system (Molecular Imaging) equipped with an $8 \times 8\ \mu m^2$ scanner. Magnetic-AC (MAC) mode (a noncontact mode) was used for all the AFM images. MAC lever, a silicon nitride based cantilever coated with magnetic film, was used as tips. FT-IR spectra were recorded on a Nicolet Nexus 870 step-scan spectrometer using a grazing incidence (Smart Refractor, Nicolet) attachment courtesy of Thermo-Nicolet Research Laboratories, Madison, WI. Polarization modulation infrared reflection absorption spectroscopy (PM-IRRAS) measurements were made on Au-coated glass substrates. The light was reflected from the samples at an 80° angle and collected over 256 scans at a spectral resolution of $4\ cm^{-1}$. Measurements were also taken with the blank ITO substrate. Surface plasmon spectroscopy (SPS) on Au-coated glass (48.6 nm) was performed using a commercially available instrument (Multiskop) with a Kretschmann configuration and attenuated total reflection (ATR) conditions.[14] The reflectance was monitored with a p-polarized He−Ne laser (632.8 nm) as a function of angle of incidence. An Al Kα X-ray source (1486.6 eV) was applied to record X-ray photoelectron spectroscopy (XPS) using a Kratos Axis 165 spectrometer. Both low (FAT, pass energy = 160 eV) and high resolution (FAT, pass energy = 40 eV) spectra were recorded.

Materials. Commercially available reagents and solvents for synthesis were all purchased from Aldrich. NMR data and chromatography were used to verify reagent integrity and purity. The solvents used for electropolymerization and the pyrrole comonomer were freshly distilled before use.

Synthesis of pyrrolyl potassium salt:[15] 8.0 g of potassium metal were dissolved in 100 mL of boiling xylene with constant stirring. After the suspension was cooled, 2 drops of absolute ethanol were added followed by addition of 13.4 g of freshly distilled pyrrole in small portions, allowing the reaction to subside between each addition. 5.0 g of excess pyrrole was added, and the mixture was refluxed for 1 h. 18.0 g of pyrrolyl potassium salt was obtained by filtration and was dried under vacuum.

Synthesis of 1-Undec-10-enyl-pyrrole. 7.9 g of pyrrolyl potassium salt and 11.6 g of 11-bromo-1-undecene were dissolved in a mixture containing 15 mL of dimethyl sulfoxide (DMSO) and 10 mL of tetrahydrofuran (THF). This was stirred for 48 h in a closed system. The excess pyrrolyl potassium salt, potassium bromide (KBr), and DMSO were separated using water, and the organic layer was treated with ethyl acetate to recover 5.5 g of the product. This was then purified using column chromatography. ^{1}H NMR: δ (ppm) 6.62 (s, 2H), 6.12 (s, 2H), 5.80 (m, 1H), 5.01 (t, 2H), 3.85 (t, 2H), 2.01 (m, 2H), 1.77 (p, 2H), 1.35 (s, 12H).

Scheme 1. Synthesis and Cross-Linking Scheme of the Polymethylsiloxane−Pyrrole Polymer, Poly(methyl-(undec-pyrrole-1-yl-decyl)-siloxane), and Pyrrole Comonomer via the Electrochemical Method

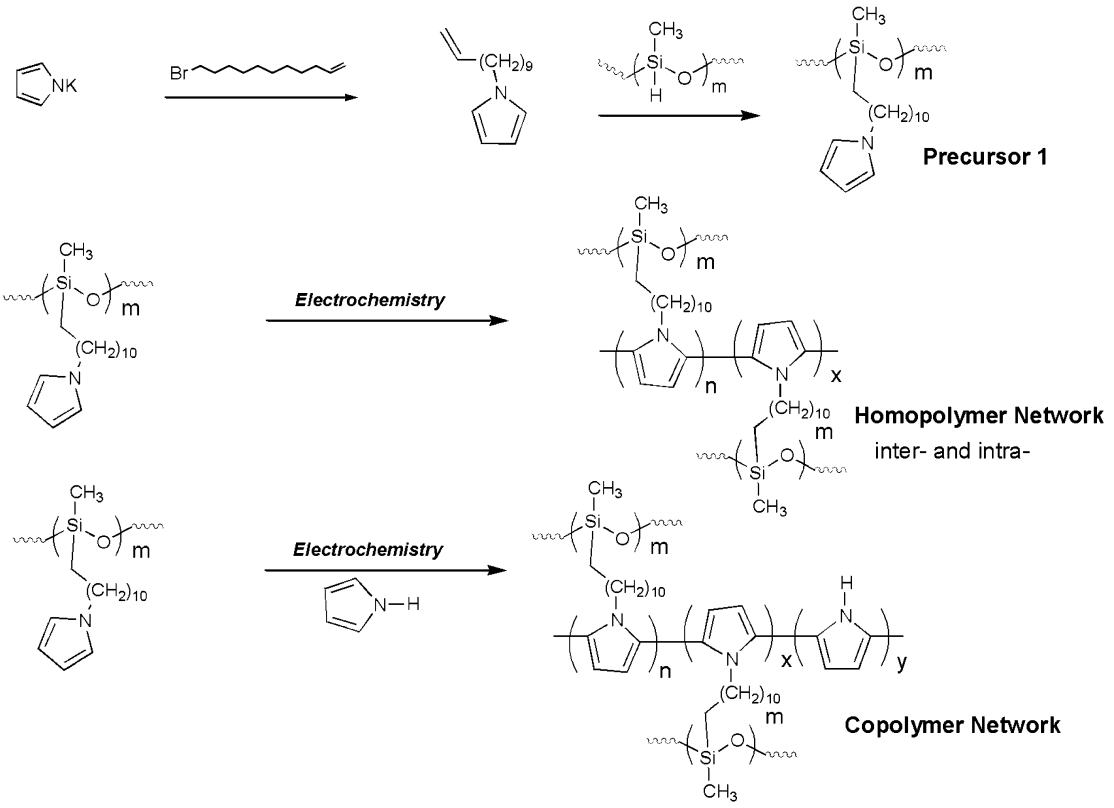

Synthesis of Poly(methyl-(undec-pyrrole-1-yl-decyl)-siloxane) or Precursor 1.[16,18] The hydrosilation reaction was done by taking 1.6 g of 1-undec-10-enyl-pyrrole and 0.4 g of poly-(meythylhydrosiloxane) with M_n = 2270 (Aldrich data, see Supporting Information). 0.007 g of the H_2PtCl_6 catalyst was added under nitrogen atmosphere in 10 mL of methylene chloride (CH_2Cl_2). The mixture was sonicated for 3 h under nitrogen atmosphere until NMR showed no Si−H proton signal at δ (ppm) 4.72 (d, 1H). The mixture was then poured dropwise into methanol to separate polymer and starting materials, thereby yielding 1.5 g of the product. ^{1}H NMR: δ (ppm) 6.62 (s, 2H), 6.12 (s, 2H), 3.85 (t, 2H), 2.01 (m, 2H), 1.24 (s, 17H), 0.50 (p, 2H), 0.06 (s, 3H).

Electrochemical Synthesis of Cross-Linked Polymer. Precursor 1 was electropolymerized and cross-linked (Figure 1) on ITO, which is the conducting electrode for CV. The ITO was pretreated using the RCA recipe ($H_2O/H_2O_2/NH_3$: 15.1 g/26.6 g/8.57 g).[17] Au-coated glass (48.6 nm) was also used as an electrode (precleaned with ion plasma cleaning under Ar, March Instruments). The same substrate was used for SPS measurements. In a three-electrode cell, a 0.020 M solution of precursor 1 and 0.086 g of tetrabutylammonium hexafluorophosphate (TBAH) as supporting electrolyte in 15 mL of methylene chloride (CH_2Cl_2) were added. The voltage was swept at the rate 100 mV/s from −800 to 1100 mV using Ag/Ag^+ as a reference electrode. After several cycles the substrate was taken out, rinsed thoroughly with CH_2Cl_2, and then dried under an N_2 flow. Polypyrrole, 0.02 M pyrrole monomer, was also electropolymerized using the same conditions.

Electrochemical Synthesis of Copolymers. In-situ electrochemical copolymerization (Scheme 1) of precursor 1 with pyrrole can be realized, since the precursor polymer deposits at a higher potential (*N*-alkylpyrrole vs pyrrole). To optimize properties closer to those of a π-conjugated polymeric system, the precursor polymer was electropolymerized with pyrrole at different composition ratios under CV conditions. This was done electrochemically using 0.02 M solutions of the following mole % compositions: (a) 5% pyrrole and 95% PP; (b) 10% pyrrole and 90% PP; (c) 25% pyrrole and 75% PP; (d) 50% pyrrole and 50% PP; (e) 100% pyrrole. In principle, this should result in a statistical mixture of cross-linked and linear species of polypyrrole within the film.

Results and Discussion

Synthesis. The overall synthetic scheme is shown in Scheme 1. Alkene-terminated pyrrole momomer units were synthesized by *N*-alkylation of pyrrole. The soluble precursor polymer was then made by hydrosilation of modified pyrrole with PMHS. Hydrosilation reactions using H_2PtCl_6 catalyst are very efficient. By NMR, completion of the reaction results in a complete disappearance of the Si−H peak at δ (ppm) = 4.72 (see Supporting Information).[16,18] SEC analysis of precursor 1 showed molecular weight values of $\bar{M}_n$ = 12 900, $\bar{M}_w$ = 43 600, $\bar{M}_z$ = 85 700, and $\bar{M}_w/\bar{M}_n$ = 3.38. However, by NMR peak integration the value is closer to $\bar{M}_n$ = 8567 g/mol, with the degree of polymerization, n = 30 (see Supporting Information). Absolute MW determination is necessary to compare the degree of polymerization more accurately between PMHS and precursor 1 in relation to the percentage of grafting. Nevertheless, the increased MW values and NMR data are consistent with the grafting of *N*-alkylpyrrole to the PMHS polymer and the absence of cross-linking reactions. The polymer was stable under ambient temperature and air conditions and easily forms CH_2Cl_2 solutions. Thus, the properties of this precursor polymer are typical for a low MW silicone polymer with functionalized side groups.[18]

Electropolymerization. Electrochemistry is a widely accepted method for in-situ polymerization of conjugated polymers on electrodes.[1] This includes potentiostatic or dynamic voltammetry methods. It is an important tool for

(17) Magnus, P.; Friend, R.; Greenham, N. *Adv. Mater.* **1998**, *10* (10), 769.
(18) Thorpe, A.; Peters, V.; Smith, J.; Nevell, T.; Tsioukis, J. *J. Fluorine Chem.* **2000**, *104*, 37.

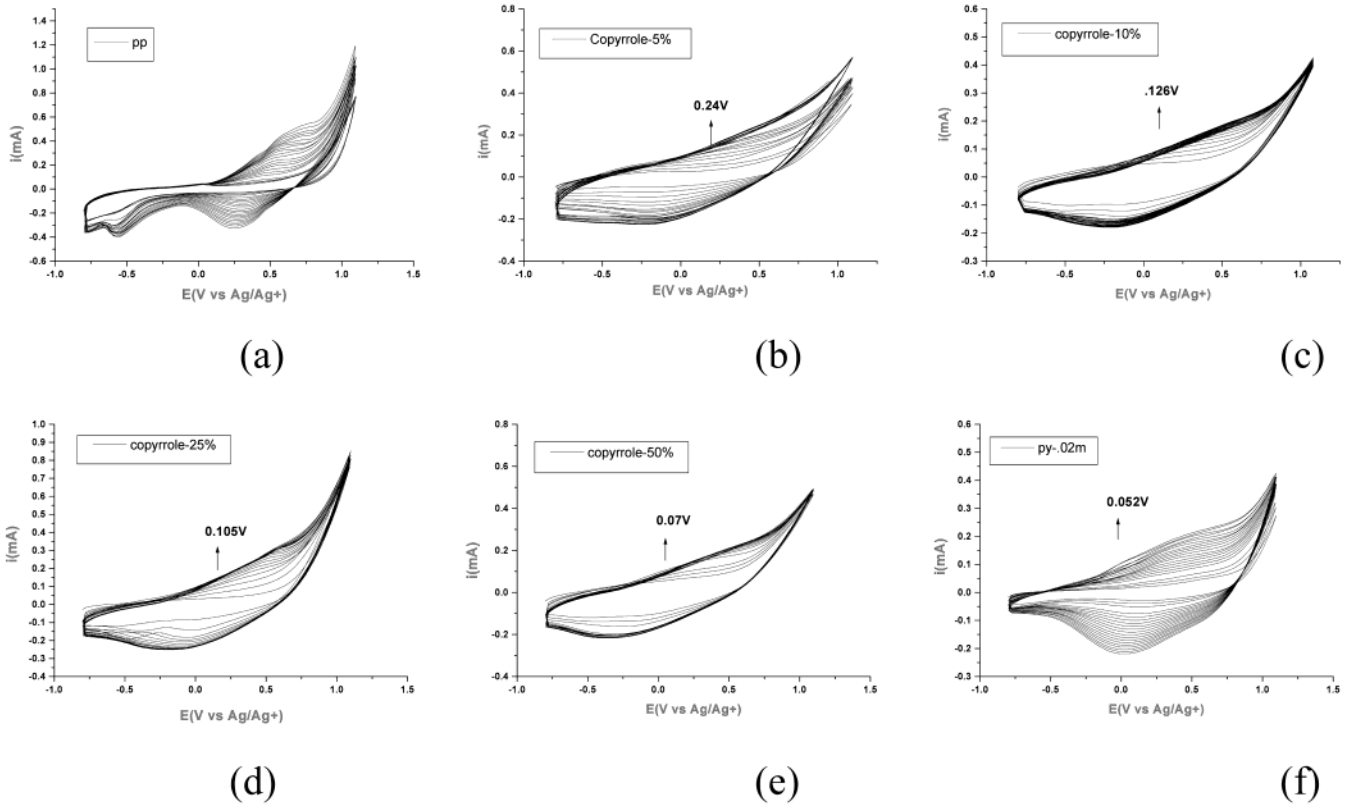

Figure 2. Cyclic voltammograms of (a) pure precursor polymer. (b) 5% pyrrole copolymer, (c) 10% pyrrole copolymer, (d) 25% pyrrole copolymer, (e) 50% pyrrole copolymer, and (f) pure pyrrole polymer (PPy).

investigating electrochemically active species involved in polymerization and doping mechanisms. The pyrrole monomer can be oxidized and coupled to form more conjugated species using CV.[19] The mechanism is via a radical cation coupling mechanism (bipolarons) at the 2 and 5 positions of pyrrole, resulting in conjugated polymer species.[1,2] In the case of electropolymerizing precursor polymers with pendant pyrrole units, an insoluble cross-linked film on a flat electrode surface is simultaneously formed (Figure 1b).[16] For this study, electropolymerization on ITO and Au (Ag/Ag^+ reference) was done with 0.02 M solutions at a scan rate of 100 mV/s for up to 30 cycles. Concentration dependent CV behavior was recently observed for this type of polymers, resulting in varying thickness and redox behavior.[16] Other conditions, such as concentration, different supporting electrolytes, potential of the substrate, electrode, potentiostatic or galvanostatic electrodepostion, and so forth, can be used to optimize the electropolymerization process.

Figure 2 shows all the CV trace diagrams from precursor 1 (Figure 2a) and varying compositions with pyrrole comonomer (mole % pyrrole on a 0.02 M concentration) in the −0.75 to 1.25 V range. The cyclic voltammograms of pure precursor 1 and PPy (Figure 2a and f) are limiting cases of the compositions. For all the CV traces, the current is initially lower on the first anodic scan but then increases rapidly at potentials sufficiently positive to initiate polymerization (onset potential). On subsequent cycles, the current increases at lower onset potentials and the oxidation and reduction peaks of the deposited film can be observed. High cyclic reversibility is also observed. The cross-linked polymers continue to grow with each additional cycle, as evidenced by integrating the area under each CV trace. A layer-by-layer growth on this type of films has been reported, and their homogeneity and thickness have been characterized by SPS on Au (as discussed later).[16] From the CV traces, it is evident that different composition ratios show mixed behavior between the limiting cases precursor 1 and PPy.

The shape of the CV trace for 100% precursor 1 (Figure 2a) is different from those for other compositions. Although the oxidation onset was first observed at 0.4 V in the anodic scan, two reduction peaks were observed at −0.6 and 0.25 V on the cathodic scan with subsequent cycles. The former peak at −0.6 V disappears with increasing pyrrole content. The latter peak at 0.25 V increases with pyrrole content. A priori, we hypothesize the two peaks to be attributed to formation of two dominant electrochemical species at this potential sweep range (−0.8 to 1.25 V): (1) coupled pyrrole (0.25 V) and (2) uncoupled pyrrole (−0.6 V). In a radical cation polymerization mechanism, reacting species of PPy (pyrrole monomer, dimers, tetramers, etc.) will form bipolarons.[2] The reactive free radical (radical cation) couples with similar groups to form covalent bonds, forming bipolarons with two cations and followed by proton loss, resulting in increased π-conjugation. However, uncoupled free radical polarons (with respect to similar pyrrole units) can also form covalent bonds with other chemical species in solution, resulting in new redox peaks.[20,21] We therefore believe that the tethered-monomer structure of precursor 1 (tethered pyrrole) and trace water or HCO_3^- (dissolved CO_2) are largely responsible for the irreversible reduction peak at −0.6 V. This property, which can be induced in other polypyrrole systems,[21] is inherently unique for precursor 1. The polymer microstructure and overoxidation phenomena result in more uncoupled

(19) (a) Li, J.; Wang, E.; Green, M.; West, P. E. *Synth. Met.* **1995**, *74*, 127. (b) Kim, D.; Hoi, J.; Kim, S.; Cho, N.; Kim, C. *Synth. Met.* **1997**, *84*, 161. (c) Lee, J.; Kim, D.; Kim, C. *Synth. Met.* **1995**, *74*, 103.

(20) Schlenoff, J.; Xu, H. *J. Electrochem. Soc.* **1992**, *139*, 2397.

(21) Novak, P.; Rasch, B.; Vielstich, W. *J. Electochem. Soc.* **1991**, *138*, 3300.

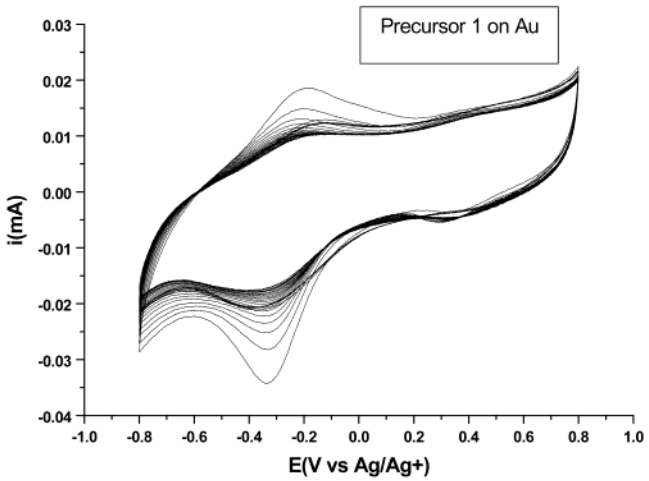

Figure 3. CV diagram on Au at (−0.8 to 0.8 V) 100 mV/s; TBAH in a 0.02 M solution of methylene chloride.

pyrrole that is easily overoxidized at the right conditions. The presence of relevant carbonyl peaks in the FT-IR spectra as a result of overoxidation is discussed in the FT-IR section (Figure 10). The rest of the results and discussions in this section should provide support for this hypothesis.

First, to differentiate substrate and overoxidation effects on the electropolymerization process, CV experiments were also performed on Au substrates at a different potential range (−0.8 to 0.8 V). From Figure 3, only one peak was observed for both oxidation and reduction processes at −0.21 and −0.35 V, respectively. This CV behavior is very similar to that previously reported for normal PPy and *N*-alkyl PPy polymerization and redox behavior (Ag/AgCl) on ITO and Pt substrates.[15,19,20] This indicates that *no* overoxidation is observed if polymerization is done below 0.8 V, consistent to what has been reported for PPy in Ag/AgCl.[21] Note that overoxidation can be a function of the ions (electrolyte) used, the concentration of O-containing species, and the reference electrode.[20,21] Thus, the dominant electrochemical process under these conditions should just be that of coupled pyrrole, that is, coupling of polaron radical cation units forming conjugated species. This has the consequence though of forming very thin layers based on a much smaller current density per cycle (SPS data) where a not so linear area increase per cycle (Figure 3) is evident compared with the case of ITO (Figure 2a).

Second, from the CV diagrams in Figure 2, the reduction and oxidation peaks shift with each cycle and with different composition ratios. In particular, the onset potential and oxidation peak shift is very strong for precursor 1 and levels off with increasing pyrrole comonomer content. Also notice the higher amount of current, *I* (mA) for precursor 1 compared to the other compositions. All this can be attributed to a more heterogeneous electron-transfer kinetics, *IR* drop of the film ($V_{total} = V_{across\ film} + I(R_{film} + R_{soln})$), and decrease of the film conductivity on going from precursor 1 to PPy.[22] The siloxane component in precursor 1 can be considered an insulating material, decreasing the amount of electroactive pyrrole units (at the same concentration) available for electrochemical coupling and formation of redox species. As deposition proceeds with higher cycles, the film grows thicker, causing a significantly higher *IR* drop for precursor 1 compared to other compositions, that is, with more redox active species or free pyrrole units. Thus, deposition becomes limited by mass transport of electrolyte ions between redox species

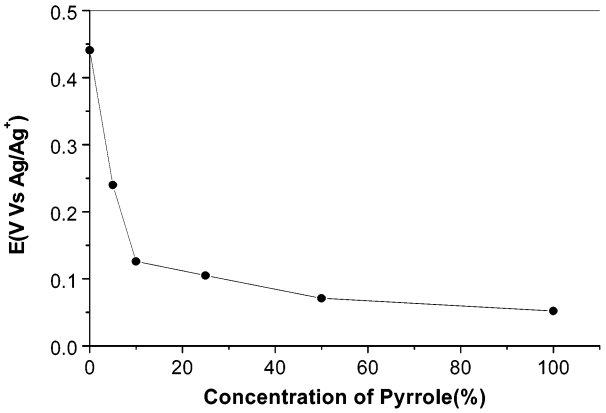

Figure 4. Trend of onset voltage with varying concentration of pyrrole copolymerized with precursor polymer.

from electrode and solution, resulting in a shift to higher potentials. Figure 4 shows the trend in onset oxidation potential with different composition ratios. The oxidation onset shifts from 0.45 V for precursor 1 to 0.052 V for PPy (Figure 4). A drop in the onset potential was observed with increasing pyrrole content. The 50% pyrrole copolymer (0.07 V) is nearer to that of PPy (0.05 V) while the 5% pyrrole copolymer (0.24 V) is nearer to the precursor polymer (0.45 V). Note that the reduction peak at −0.6 V in precursor 1 starts to disappear even with 5% pyrrole added. The slope in this potential region changes with composition until a prominent peak is observed at 0.01 V for PPy in the cathodic scans. The higher oxidation onset with precursor 1 also verifies the fact that the silicone polymer backbone promotes a high degree of network formation (cross-linked vs linear polypyrrole), reducing overall film swellability.[10] Changing composition changes the formation of linear versus cross-linked polypyrrole species, affecting both the electrochemical and morphological (as discussed in the next section) properties of the film.

Last, in the absence of overoxidation with Au substrate (Figure 3), precursor 1 forms very thin layers for each cycle, as monitored by SPS. SPS is a technique of high sensitivity for characterization of ultrathin films at the sub-nanometer thickness scale.[14] It is a powerful tool for probing optical and dielectric properties at the nanoscale. By monitoring angular-reflectivity changes before and after polymerization, we were able to obtain information on film formation and the optical properties. The resonance angle and shape of the curves are well correlated to film thickness and dielectric constants, that is, refractive index, by the Fresnel formalism. Figure 5 shows the SPS curves for precursor 1 deposited on Au-coated glass substrates in an ATR experiment. Immediately noticeable is the plasmon curve shift to higher incidence angles, indicating a general increase in thickness for each cycle. A thickness of 5.8 nm was calculated on deposition with Au at 30 CV cycles. This thickness is *very thin* compared to what has been previously reported with another polysiloxane precursor polymer, for example, ∼76 nm after 11 cycles and the electrodeposited films on ITO (Table 1).[16a] On the basis of the current density (*i*) and CV behavior in Figure 3, this is not surprising. By comparing the relative current density differences and area increase per cycle (comparing Figures 2a and 3), it should be possible to extrapolate much thicker films of precursor 1 on ITO.[16a]

Thus, all these observations support the fact that electropolymerization of precursor 1 above 0.8 V versus Ag/AgCl results in thicker cross-linked films with overoxidation of uncoupled pyrrole. Polymerization below this

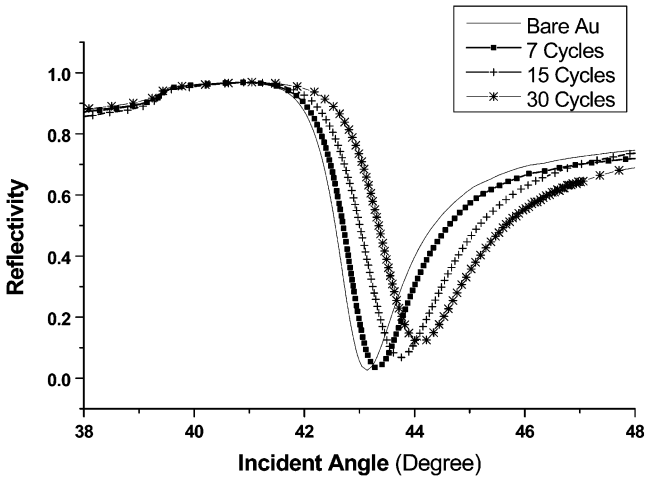

Figure 5. SPS reflectivity data of CV electropolymerized film on Au at (−0.8 to 0.8 V) 100 mV/s; TBAH in a 0.02 M solution of methylene chloride.

Table 1. Thickness and Root-Mean-Square Roughness Data from AFM[a]

PPy/precursor-1 ratio	thickness (nm)	rms roughness (nm)	no. of cycles (CV)
0:100	200	8.5	30
5:95	180	4.9	30
50:50	100	3.0	20
100:0	70	7.0	30

[a] Thickness was determined by AFM profilometry directly on the ITO surface, and the method is discussed in the Supporting Information. Roughness was calculated from a $3 \times 3\ \mu m^2$ image.

potential will result in very thin deposited films. Overoxidation occurs with precursor 1 because not all the pyrrole units are able to cross-link or react because of reduced conformational and translational mobility due to tethering (Figure 1). As a result, uncoupled radical cations will rather react with dissolved CO_2 and H_2O impurities, forming oxidized pyrrole species above the overoxidation potential limit.[21] However, to form thickly deposited films, this is necessary, since it optimizes coupling of all the pyrrole units at ambient air conditions (studies should be performed in inert conditions for comparison). As discussed in the next section, this has resulted in some unusual morphologies.

Morphology Studies and Thickness Profilometry by AFM. The most interesting features of these films relate to morphology after electropolymerization and at different composition ratios. Interesting phase-separated domains were observed on the films formed, especially after 30 CV cycles. Figure 6 shows the AFM topological and phase images with varying compositions of the electropolymerized precursor polymer and the pyrrole comonomer. We did not observe these features on electropolymerized films below the 20−25th cycle on both Au and ITO substrates. The AFM image after 30 CV cycles on an Au electrode (−0.8 to 0.8 V) for precursor 1 is also shown (Figure 6e) for comparison. The morphologies are very different when the CV cycles are below the overoxidation potential threshold. In general, there is a change in roughness and morphology on going from pure precursor 1 to PPy. Pure PPy, which shows electrical conducting properties as oxidized and doped films,[1] has been extensively investigated, but not with regard to the morphologies as deposited ultrathin films. Rough morphologies with electropolymerization are a consequence of the growing polymer chain precipitating out of solution and depositing on the electrode surface.[9] In general, the mechanism of film deposition is as follows: at the onset of oxidation, the formation and coupling of pyrrole radical cations occurs, forming oligomers, which eventually precipitate at random sites on the electrode surface. These formed nucleation sites enhance polymer growth outward from the electrode surface (one-dimensional nucleation), in layered sheets (two-dimensional nucleation), or by amorphous growth (three-dimensional nucleation).[23]

In these films, electropolymerization of polymethylsiloxane-functionalized pyrrole resulted in the formation of phase-separated domain structures that are regular in feature. We observed the formation of these nanoscale "dots" of the order of 150−200 nm in diameter for pure precursor polymer. The size of these dots decreased with increasing pyrrole comonomer content from 100−150 to 50−100 nm ranges for 10% and 50% compositions, respectively (see Supporting Information), and the distribution becomes broader (Figure 6). As a consequence of protruding dots, the morphology of precursor 1 is more textured compared to those for the 50% pyrrole composition and the pure pyrrole. The absence of the dots on PPy (globular morphology) can be confirmed from the images. The root-mean-square (rms) roughness of the films is summarized in Table 1. The rms roughness values for precursor 1 and the copolymers are skewed by the presence of the dot textures. However, comparison of the surface around the dots and the texture based on the phase images (right image) indicates that these are morphologically smoother films.

These dots can be attributed to low cross-linking at the surface of precursor polymer pyrrole units, resulting in phase segregation at the surface, especially with thicker films. The fact that the size and amount of dots decreases with increasing pyrrole monomer content verifies the effect of polysiloxane on film morphology. The interaction parameter (χ) between polysiloxane and cross-linked polypyrrole, the low glass transition temperature (T_g), and the surface energy (γ) all play an important role in understanding the observed morphology trends.[24] With electropolymerization, especially at higher cycles, the film becomes sufficiently thick so that it begins to block the electron transfer between electrode, polymer film, and solution interface, that is, the large *IR* drop. This will result in a decreased extent of cross-linking at the outer layer or interface where un-cross-linked tails and loops phase segregate from the cross-linked regions, that is, result in dewetting (Figure 7).[25] This explains the circular domain-like morphologies observed under AFM, which were not observed with thinner films (lower cycles and on Au substrates at −0.8 to 0.8 V). Thus, formation of these dots is dominated by the volume ratio of polymethylsiloxane chains, becoming smaller with lower precursor 1 content in the different compositions.

(22) (a) Ferraris, J. P.; Haillon, T. R. *Polymer* **1989**, *30*, 1319. (b) Yassar, A.; Garnier, F. *Macromolecules* **1989**, *22*, 804. (c) Wei, Y.; Chan, C. C.; Tian, J.; Jang, G. W.; Hseuh, K. F. *Chem. Mater.* **1991**, *3*, 888.

(23) (a) Downard, A. J.; Pletcher, D. *J. Electroanal. Chem.* **1986**, *206*, 245. (b) Li, F.-B.; Albery, W. J. *Langmuir* **1992**, *8*, 1645. (c) Hillman, A. R.; Mallen, E. F. *J. Electroanal. Chem.* **1987**, *220*, 351. (d) Beck, F.; Oberst, M. *Makromol. Chem., Makromol. Symp.* **1987**, *8*, 97. (e) Rishpon, J.; Redondo, A.; Derouin, G.; Gottesfeld, S. *J. Electroanal. Chem.* **1990**, *294*, 73. (f) Baker, C. K.; Reynolds, J. R. *J. Electroanal. Chem.* **1988**, *251*, 307. (g) Marcos, M. L.; Rodriguez, I.; Gonzalez-Velasco, J. *Electrochim. Acta* **1987**, *32*, 1453. (h) Hamnett, A.; Hillman, A. R. *J. Electrochem. Soc.* **1988**, *135*, 2517.

(24) (a) Rockford, L.; Mochrie, S.; Russell, T. *Macromolecules* **2001**, *34*, 1487. (b) Mansky, P.; Harrison, C.; Chaikin, P.; Register, R.; Yao, N. *Appl. Phys. Lett.* **1996**, *68*, 2586. (c) Elias, H.-G. *Macromolecules*, 2nd ed.; Plenum: New York, 1984.

(25) (a) Wang, C.; Krausch, G.; Geoghegan, M. *Langmuir* **2001**, *17*, 6269. (b) Henn, G.; Bucknall, D. G.; Stamm, M.; Vanhoorne, P.; Jerome, R. *Macromolecules* **1996**, *29*, 4305.

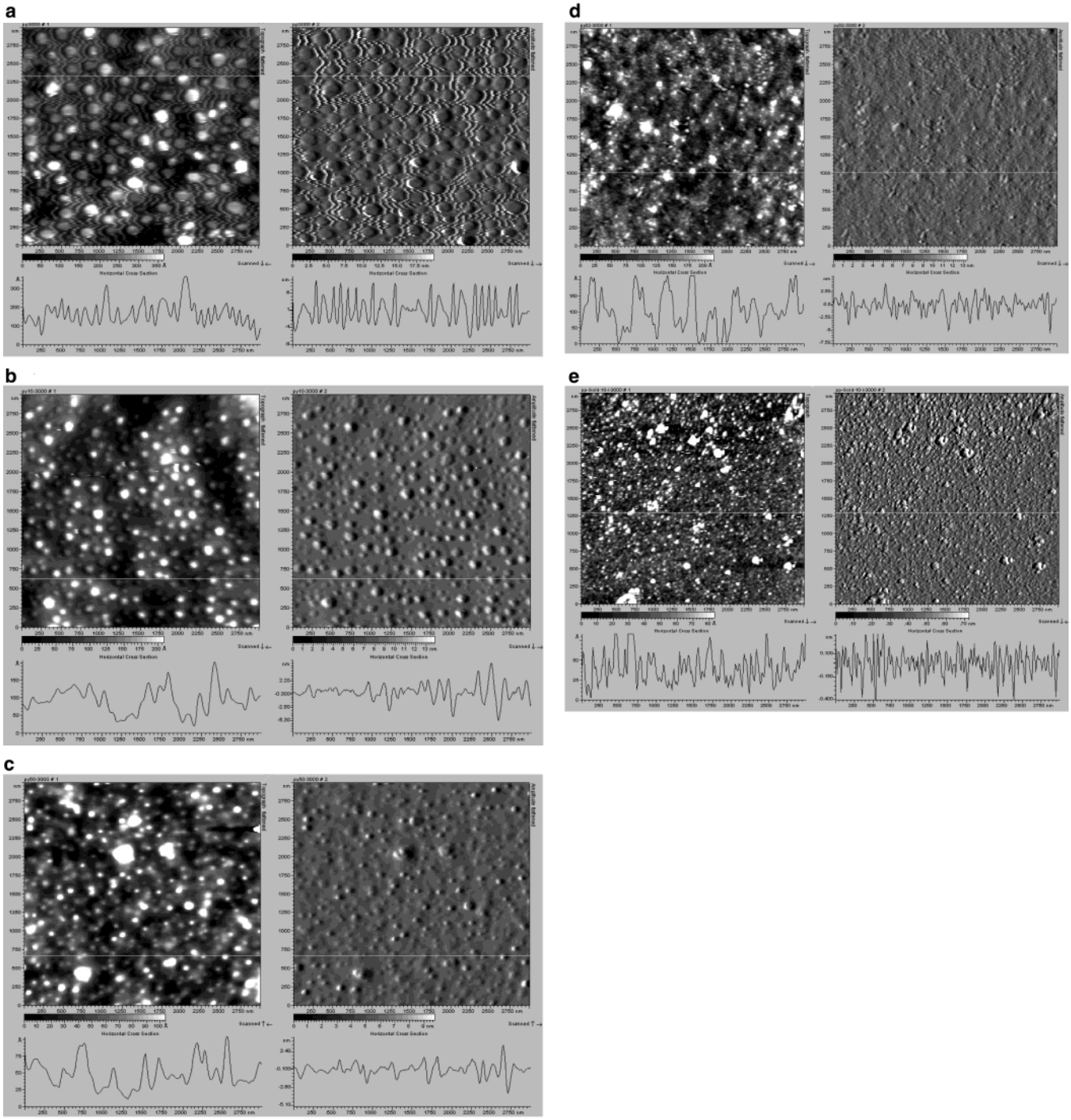

Figure 6. AFM images ($3 \times 3\ \mu m^2$ scan) of (a) pure precursor polymer, (b) 10% pyrrole copolymer, (c) 50% pyrrole copolymer, (d) pure polypyrrole, and (e) precursor 1 on an Au electrode.

The differences in the mechanism of electropolymerization between a precursor polymer and a small molecule monomer may also provide some important explanation.[9] Morphology studies of previously cross-linked poly(methyl-(10-thiophen-3-yl-decyl)siloxane)[16a] and poly(6-pyrrol-1-yl-hexyl methacrylate)[26] did not show these features. In particular, for poly(methyl-(10-thiophen-3-yl-decyl)siloxane), the film became more insulating with higher number of cycles, preventing electropolymerization up to the 20th cycle. Also, the differences in the χ parameter and surface energy may not be sufficient to result in phase segregation, although a more membrane-like morphology was observed.[16a] Direct polymerization of pyrrole to form PPy films did not show this morphology.[25] Clearly, more experiments can be done, including SEM and TEM imaging and annealing, in order to understand these unique morphologies together with their electropolymerization conditions.

Using AFM profilometry, the total thicknesses of the electrodeposited films were determined directly from the ITO surface (see Supporting Information). The thickness values are summarized in Table 1. As discussed earlier, film thickness should increase linearly with the number of CV cycles, on the basis of increasing current density differences and the area increase of the CV curves (Figure

(26) (a) Deng, S.; Advincula, R. *Polymer Prepr.* (*Am. Chem. Soc., Div. Polym. Chem.*), **2002**, *43*, 106. (b) Deng, S.; Advincula, R. *Chem. Mater.*, submitted.

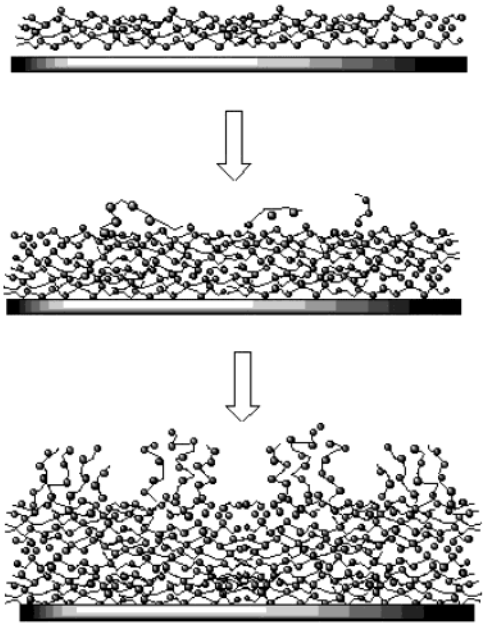

Figure 7. Schematic diagram of the formation of dot structures on the surface resulting from phase segregation of siloxane domains.

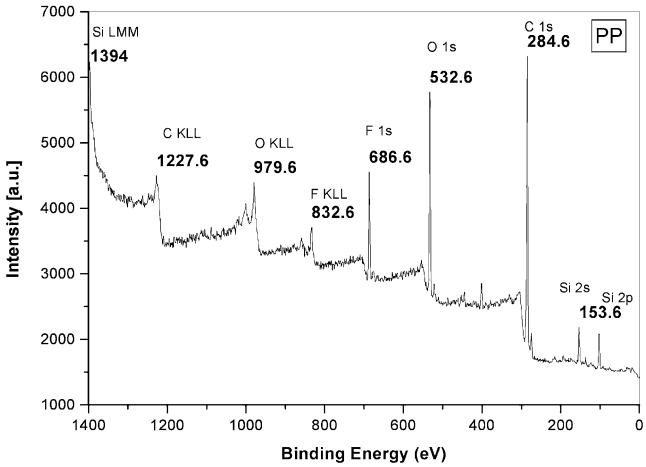

Figure 8. Survey scan of XPS spectra for the precursor polymer, indicating the presence of relevant peaks using the Al Kα X-ray source (1486.6 eV; FAT, pass energy = 160 eV).

2). The rate of this increase varies with the composition ratio of precursor 1 and PPy on the film. In general, a higher precursor 1 content results in thicker films.

XPS Investigations. Figure 8 shows XPS spectra for electropolymerized precursor 1. The carbon component, C 1s (284.5 eV), shows the most intense peak together with the peaks of Si, N, O, and F in the low resolution XPS spectra. The Si peaks at Si 2p 100.8 eV and Si 2s 153.6 eV are normal for the polysiloxane Si−O and Si−C bonds, indicating the absence of side reactions that may be attributed to degradation during the electrochemical process. The other peaks are N 1s (398 eV) and O 1s (532.6 eV). The presence of fluorine, F 1s 686.6 eV, with a higher photoelectron transition sensitivity factor in XPS, signifies that washing the films after electropolymerization did not remove all TBAH counteranion electrolytes.

Figure 9a shows background subtracted high-resolution C 1s XPS spectra of a precursor 1 film, which was fitted to three components using a standard line shape analysis with a Gaussian fitting function. Figure 9b shows the N 1s XPS spectra for 10% copolymer under the same

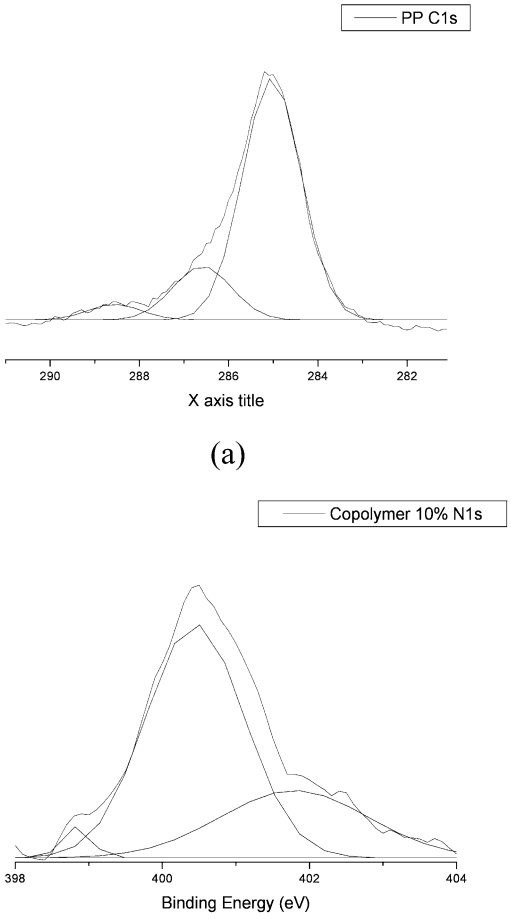

Figure 9. (a) High resolution C 1s XPS spectra of the precursor polymer and (b) for N 1s of 10% copolymer.

Table 2. XPS Data Showing the Binding Energy for Different Elements Present in the Precursor Polymer

precursor polymer (C 1s)	binding energy	assignments
C1	284.8	C−C
C2	286.4	C−Si, C═N, C−N^+
C3	288.71	C═O
copolymer 10% (N 1s)	**binding energy**	**assignments**
N1	398.6	C═N
N2	400.59	N−H (pyrrole)
N3	401.89	C−N^+

conditions. Table 2 shows details of the high-resolution XPS spectra and the various binding energy (BE) values and chemical assignments.[27]

As mentioned, the C 1s spectrum could be fitted with three components. The component at ∼284.88 eV is attributed to C−C bonds. The derived composition of C−C is exactly the same as the theoretical composition. The component at about 286.38 eV is attributed to the C−N^+ group. We cannot exclude the C═N group on the basis of the C 1s spectrum alone because it has a binding energy that falls under that of peak C 2.[28] However, the N 1s spectrum can be conclusive in confirming its absence. The component at about 288.71 eV can be attributed to the C═O group, which confirms overoxidation during the

(27) De Benedeto, G. E.; Malitesta, C.; Palmissano, F.; Zambonin, P. G. *Anal. Chem. Acta* **1999**, *389*, 197.
(28) Malitesta, C.; Losito, I.; Sabbatini, L.; Zambonin, P. *J. Electron Spectrosc. Relat. Phenom.* **1995**, *76*, 629.

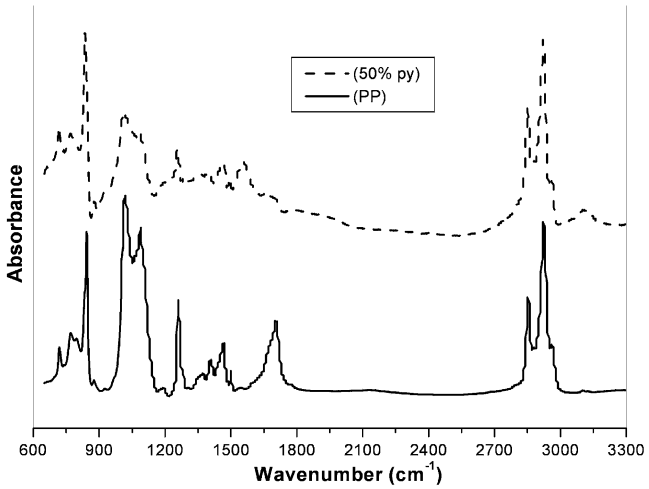

Figure 10. IR spectra of precursor 1 and the 50% copolymer of pyrrole. Note the difference in the 1700 region indicating the presence of the overoxidation peak for precursor 1.

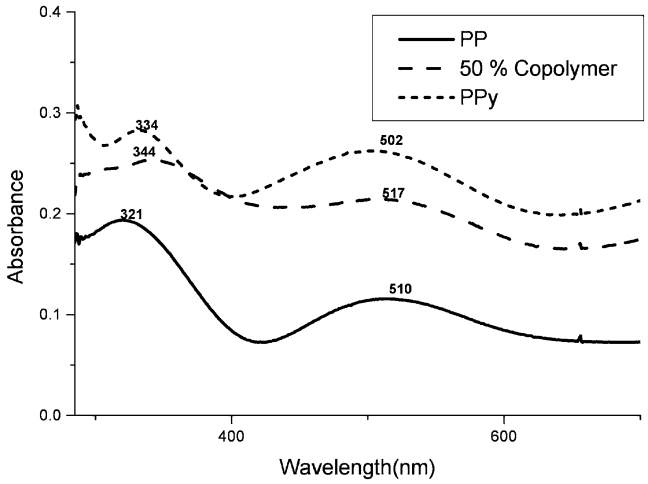

Figure 11. UV−vis spectra for the pure precursor polymer precursor 1, 50% copolymer with pyrrole,and PPy on ITO.

electropolymerization cycle for precursor 1. This was also confirmed by our FT-IR measurements. Not all films were analyzed by high resolution XPS, and it is possible that no overoxidation will be observed on other film compositions, especially since polypyrrole has a lower oxidation potential.

The N 1s spectrum for the 10% pyrrole composition could be fitted with three components.[29] The major component at ∼400.59 eV is attributable to the amine-like structure (also referred to as the neutral pyrrolylium nitrogen), and the other at ∼401.89 eV can be attributed to the positively charged nitrogen atoms (N^+) or doped structure. The peak component corresponding to the imine-like structure (C═N), which has a binding energy at approximately 398.6 eV,[30] is not found for the 10% composition. The most important conclusion though is that the 10% incorporates more polypyrrole-like structure (not *N*-alkyl pyrrole), with this film composition confirming the statistical copolymerization.

Thus, XPS spectra verify the fact that the composition at the surface is consistent with the incorporation of more pyrrole units in the copolymer and none for precursor 1, except for the *N*-alkyl pyrrole. Furthermore, the films are doped, indicating inclusion of supporting electrolyte ions on the films during the electropolymerization process, not removed by simple washing. This is consistent with both the FT-IR and UV−vis spectra observed for these polymers.

FT-IR Spectra. Figure 10 shows FT-IR spectra of precursor 1 and the 50% copolymer. A very sharp band at 1260 cm^{-1} is due to Si−CH_3 symmetric deformation, and the absorption at 860−760 cm^{-1} is due to methyl rocking or Si−C stretching[31] characteristic of the Si−CH_3 groups. The peaks from 1090 and 1020 cm^{-1} are due to the finite Si−O−Si siloxane chains. The use of higher voltage and time requirements (potentiostatic deposition) for precursor 1 leads to overoxidation of pyrrole, as discussed earlier. This resulted in a conjugate carbonyl peak observed at 1710 cm^{-1}.[20] This has previously been observed by other investigators[32] and was confirmed by our XPS measurements and the two electrochemical reduction peaks observed with precursor 1. Overoxidation should be less of a possibility by copolymerizing with pyrrole monomer, which has a lower oxidation potential. Therefore, we did not see the conjugated carbonyl peak in the 50% copolymer, as shown in Figure 10.

Figure 11 shows UV−vis spectra of the polymers where traditional bands consistent with polypyrrole can be observed. The absorbance of the blank ITO reference substrate was subtracted (absorption at 320 nm).[33] The polymer films grown on ITO showed absorbances typical of N-substituted polypyrroles. The λ_{max} of the neutral polypyrrole for the $\pi-\pi^*$ transition (normally at 334 nm) is masked by the ITO. The $n-\pi^*$ transition for the polymers is observed between 502 and 517 nm compared to 502 nm observed for polypyrrole.[34] The absorption maximum of polypyrrole is consistent with a bipolaron transition.[35] Since the polymer is not in a completely oxidized or reduced state, we see some absorbance toward the near-IR, beyond 600 nm, indicating the presence of some charged species. This is also consistent with XPS results on the oxidation and reduction states of N (pyrrole monomer). In terms of optical quality, the precursor polymer was uniformly transparent, especially for an ultrathin film. However, the films become more opaque on going from pure precursor 1 to pure PPy, that is, with increasing pyrrole monomer content. Thus, it is possible to control the optical transparency of these films by controlling the thickness and composition ratio with the pyrrole monomers.[36] Further studies are being performed to investigate the electrical conducting properties and charge carrier mobilities of these films with changing composition.

Conclusions

This work demonstrated the precursor polymer method for the synthesis and electropolymerization of polysiloxane-functionalized pyrrole or poly(methyl-(undec-pyrrole-1-yl-decyl)-siloxane) to form an insoluble conjugated

(29) Lim, V.; Kang, E.; Neoh, K. *Macromol. Chem. Phys.* **2001**, *202*, 2824.
(30) Lim, V.; Kang, E.; Neoh, K. *Synth. Mater.* **2001**, *123*, 107.
(31) Nicho, M. E.; Hu, H. *Sol. Energy Mater. Sol. Cells* **2000**, *63*, 423.
(32) Ghosh, S.; Bowmaker, G. A.; Cooney, R. P.; Seakins, M. J. *Synth. Met.* **1998**, *95*, 630.
(33) (a) Berlin, A.; Zotti, G.; Schiavon, G.; Zecchin, S. *J. Am. Chem. Soc.* **1998**, *120*, 13453. (b) Zotti, G.; Zecchin, S.; Berlin, A.; Schiavon, G.; Giro, G.; *Chem. Mater.* **2001**, *13*, 43. (c) Norris, I. D.; Kane-Maguire, L. A. P.; Wallace, G. G. *Macromolecules* **2000**, *33*, 3237.
(34) Chen, Yu.; Imrie, C. T.; Ryder, K. S. *J. Mater. Chem.* **2001**, *11*, 990.
(35) Genies, E.; Pernaut, J.; Santier, C.; Syed, A.; Tsintavis, C. *Springer Series in Solid State Sciences*, Vol. 63; Springer: Berlin, 1984; p 211.
(36) Stanke, D.; Hallensleben, M.; Toppare, L. *Synth. Met.* **1995**, *72*, 89.

polypyrrole network. CV behavior and changes in spectral properties are consistent with the formation of polypyrrole units and cross-linking of the film. Overoxidation of pyrrole units was observed but is essential for increased film thickness. Different pyrrole comonomer composition ratios resulted in varying film properties, the most interesting of which are changes in morphology. AFM images show that relatively smooth films were formed together with the appearance of phase separated "dot" structures, which changed in size and distribution with composition. XPS, FT-IR, and UV−vis spectroscopy confirmed these trends. In principle, the morphology of these films can be controlled by composition, precursor polymer design (microstructure), and electropolymerization conditions, resulting in phase behavior and domain formation at different length scales.

Acknowledgment. The authors gratefully acknowledge partial funding from NSF-CAREER (Grant DMR-99-82010), and they acknowledge Molecular Imaging Inc., Optrel, Inc., and Nicolet Research Laboratories for technical support and Dr. Earl Ada of the University of Alabama for the XPS measurements.

Supporting Information Available: Description of MW and NMR data for the precursor polymer and AFM profilometry experiments. This material is available free of charge via the Internet at http://pubs.acs.org.

LA025517Y